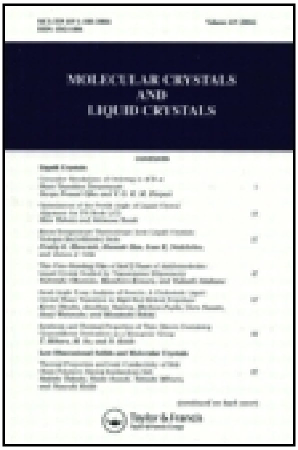

Molecular Crystals and Liquid Crystals
Publication details, including instructions for authors and subscription information:
http://www.tandfonline.com/loi/gmcl20

Some Characteristics of a Liquid-Crystal Phase Grating for THz Waves

Chia-Jen Lin [a], Chuan-Hsien Lin [a], Cho-Fan Hsieh [a], Ru-Pin Pan [a], Yu-Tai Li [b] & Ci-Ling Pan [b]

[a] Department of Electrophysics, National Chiao Tung University, Hsinchu, Taiwan, Republic of China

[b] Department of Photonics and Institute of Electro-Optical Engineering, National Chiao Tung University, Hsinchu, Taiwan, Republic of China

Published online: 05 Oct 2009.

To cite this article: Chia-Jen Lin, Chuan-Hsien Lin, Cho-Fan Hsieh, Ru-Pin Pan, Yu-Tai Li & Ci-Ling Pan (2009) Some Characteristics of a Liquid-Crystal Phase Grating for THz Waves, Molecular Crystals and Liquid Crystals, 507:1, 114-121, DOI: 10.1080/15421400903050301

To link to this article: http://dx.doi.org/10.1080/15421400903050301

Mol. Cryst. Liq. Cryst., Vol. 507, pp. 114–121, 2009

ISSN: 1542-1406 print/1563-5287 online
DOI: 10.1080/15421400903050301

Some Characteristics of a Liquid-Crystal Phase Grating for THz Waves

Chia-Jen Lin[1], Chuan-Hsien Lin[1], Cho-Fan Hsieh[1], Ru-Pin Pan[1], Yu-Tai Li[2], and Ci-Ling Pan[2]
[1]Department of Electrophysics, National Chiao Tung University, Hsinchu, Taiwan, Republic of China
[2]Department of Photonics and Institute of Electro-Optical Engineering, National Chiao Tung University, Hsinchu, Taiwan, Republic of China

We propose and demonstrate an electrically controlled liquid crystal phase grating for the terahertz wave. The performance of the device was characterized by a terahertz time-domain spectrometer. The experimental results were in a good agreement with the prediction by classic diffraction theory.

Keywords: liquid crystal; phase grating; terahertz devices; terahertz wave

INTRODUCTION

In the past decade, terahertz (THz) photonics had progressed remarkably. THz technology and its applications including ultrafast dynamics in materials, communication, biomedical imaging, and environmental surveillance were realized [1–3]. However, essential quasi-optic components such as phase shifters, modulators, attenuators, polarizers, and beam splitters in the THz range are relatively underdeveloped. For controlling electromagnetic waves, the periodic structures such as gratings are frequently employed. In the THz range, tunable devices based on optically and electrically controlled

This work was supported in part by the National Science Council grants NSC 95-2221-E-009-249, PPAEU-II and the ATU program of the Ministry of Education, Taiwan, Republic of China.

Address correspondence to Ci-Ling Pan, Department of Physics, National Tsing Hua University, Hsinchu, Taiwan 30013, Republic of China. E-mail: clpan@faculty.nctu.edu.tw

carrier concentration in quantum-well structures have been demonstrated. These tunable THz devices, however, have limited range of tunability and have to be operated at cryogenic temperatures far below room temperature [4–6]. Previously, we have reported the complex optical constants of several nematic liquid crystals in the THz frequency range [7–11]. Commonly available nematic liquid crystals, e.g., 5CB and E7, exhibit birefringences as large as those in the visible and relatively small absorption coefficient from 0.2 to 1 THz. Various tunable THz devices based on nematic liquid crystals (NLC), such as phase shifters and filters that are controlled either electrically or magnetically, have been demonstrated [12,13]. Recently, we have demonstrated a magnetically controlled phase grating for manipulating the THz wave [14]. Electrically controlled phase grating for THz wave is desirable. In this work, we propose a design of such a device and report some of its characteristics.

Operation Principles and Experimental Setups

The electrically controlled THz phase grating in this work could be seen as a binary phase grating. It contains alternate sections of two

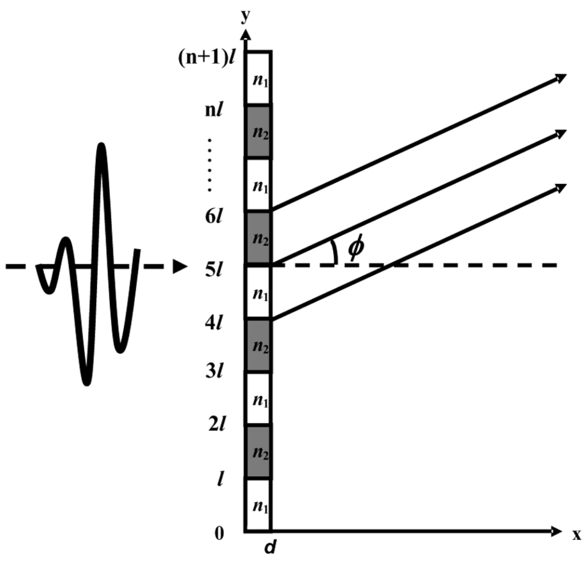

FIGURE 1 Schematic drawing of a generic binary phase grating, n_1, n_2: indices of refraction, d: depth of grating, l: width of each element, ϕ: diffraction angle. The THz pulse is normally incident on the phase grating.

materials with different refractive indices as shown in Figure 1. The electric fields of electromagnetic waves that pass through materials 1, 2 and the total field E detected at an angle of ϕ from the incident beam can be written as,

$$
\begin{aligned}
E_1(\phi) &= \sum_{\mathrm{n}=1}^{odd} \int_{\mathrm{n}l}^{(\mathrm{n}+1)l} E_0 e^{iky\sin\phi} e^{i(n_1+i\kappa_1)kd} dy, \\
E_2(\phi) &= \sum_{\mathrm{n}=0}^{even} \int_{\mathrm{n}l}^{(\mathrm{n}+1)l} E_0 e^{iky\sin\phi} e^{i(n_2+i\kappa_2)kd} dy, \\
E &= E_1(\phi) + E_2(\phi),
\end{aligned}
\tag{1}
$$

where E_0 is the amplitude of the incident electric field, ϕ is the diffraction angle, k is the wave number of the electromagnetic wave in free space, l is the width of each material, d is the thickness of the grating, and $n_1+i\kappa_1$ and $n_2+i\kappa_2$ are complex refractive indices of materials 1 and 2, respectively.

The grating was designed such that the efficiency of the 0th order diffracted THz waves would be highest around 0.3–0.5 THz. Parallel grooves having a period of 2.0 mm, a width of 1.0 mm, and a groove-depth of 2.5 mm were fabricated by stacking ITO (indium-tin-oxide) film coated fused silica substrates, for which the refractive index is 1.95 in the THz frequency region (0.2–0.8 THz). The surfaces of the fused silica were coated with polyimide (SE-130B, Nissan) and rubbed for alignment. The grooves were filled with the NLC, E7 (Merck), and sealed with a sheet of fused silica coated with DMOAP. Therefore, this device was constructed with alternate sections with 1.0 mm thick NLC layer and 1.0 mm thick fused silica sheet. The dimension of the NLC layers was 20.0 mm $\times$ 2.5 mm $\times$ 1.0 mm. In previous work, we have shown that the LC layer as thick as 1.5 mm can have a good alignment [13].

A schematic illustration of the device and the relationship between the NLC director and applied electric field are shown in Figure 2. The NLC E7 was aligned along the x-direction by the alignment layer. Since E7 is a birefringent material with positive dielectric anisotropy, the molecules tend to be aligned parallel to the direction of the applied electric field when the applied voltage is lager than the threshold voltage. The complex refractive indices of E7 in the THz frequency range have previous reported by our group [12]. There are no resonances from 0.2 to 1.2 THz. The value of the real part of the refractive indices for the ordinary wave and the extraordinary wave are respectively 1.58 and 1.71. The corresponding imaginary indices are

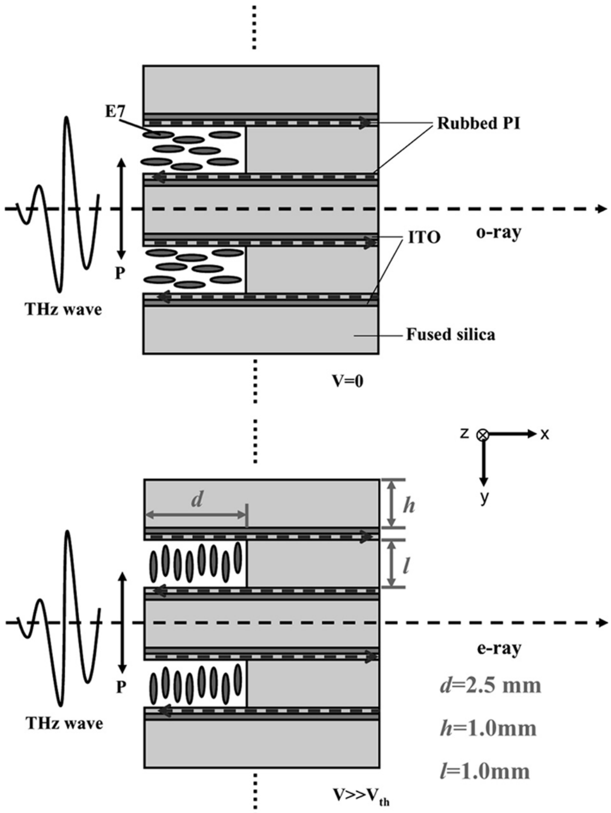

FIGURE 2 Schematic illustration of electrically controlled NLC based THz phase grating. The polarization and propagation direction of incident THz wave are parallel to y- and x-axis, respectively. The director of NLC is rotated from x- to y-axis with increasing applied bias. ITO: indium-tin-oxide film as electrode, P: polarization of THz wave, V: bias, V_{th}: threshold voltage. The dimensions of the structure are shown.

κ_o (0.010) to κ_e (0.007). The effective refractive index of NLC experienced by the THz propagating through the device can be written as

$$n_{eff} = \left(\frac{\cos^2 \theta}{n_o^2} + \frac{\sin^2 \theta}{n_e^2} \right)^{-1/2}, \tag{2}$$

where n_o and n_e are ordinary and extraordinary indices of refraction of NLC and θ is the reorientation angle of NLC molecules from the original orientation. A stack of ITO film coated fused silica sheets without

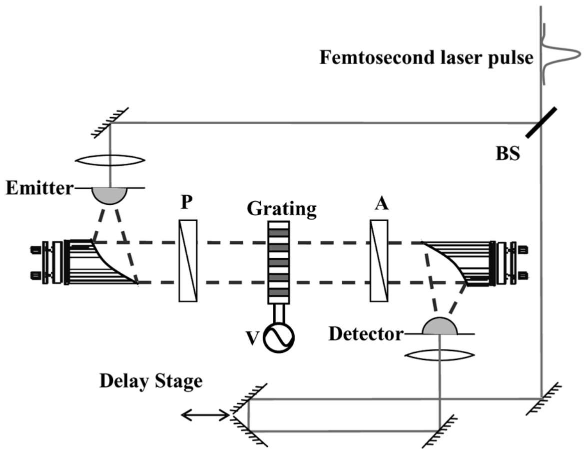

FIGURE 3 Schematic diagram of the THz-TDS system. P: polarizer, A: analyzer, BS: beam splitter, V: bias. Dashed line indicates the propagation trace of the THz wave.

filling NLC, identically in dimension to that of the grating was prepared as the reference. The data presented below, were obtained at room temperature $23 \pm 0.5°C$.

A photoconductive antenna-based terahertz time-domain spectrometer (THz-TDS) [15] was utilized to measure the 0th order diffraction spectra of the device. This is shown in Figure 3. Briefly, the pump beam from a femtosecond mode-locked Ti:sapphire laser illuminated a dipole antenna fabricated on low-temperature-MBE-grown GaAs to generate the broadband THz signal, which was collimated and collected through the THz phase grating by off-axis parabolic gold mirrors. A pair of parallel wire-grid polarizers (Specac, No. GS57204) was placed before and after the device under test. The 0th order diffracted pulse of THz radiation was coherently detected by another photoconductive antenna of the same type gated by ultrafast pulses from the same laser.

RESULTS AND DISCUSSIONS

The 0th order diffracted THz pulses transmitted through the phase grating for both ordinary and extraordinary waves and that of the reference (black, red, and blue curves) were presented in Figure 4. The applying voltages are 0 and $90\,V_{rms}$ for o-ray and e-ray, respectively. An oscillating component can be seen arriving 3.0 ps and

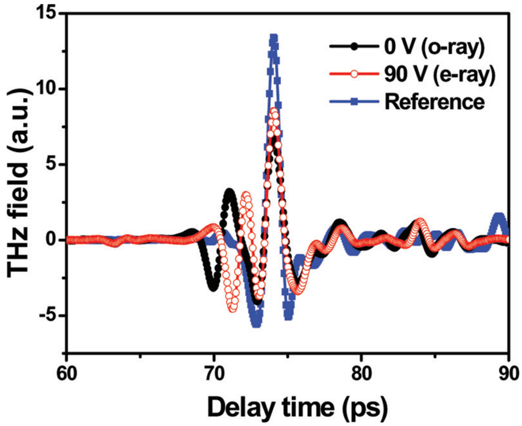

FIGURE 4 Temporal profiles of the 0th order diffracted THz pulses through the phase grating bias at 0 V (o-ray) and 90 V (e-ray) and that of a reference sample.

1.9 ps before the main pulse for ordinary and extraordinary waves, respectively. This is attributed to the propagation time difference between the waves through fused silica and NLC. The calculated delay times, $\delta nd/c$, where δn is the difference of the refractive indices between fused silica and NLC, d is groove depth and c is the speed of light in vacuum, are 3.1 ps and 2.0 ps for o- and e-ray, respectively. These are very close to the experimental observed time difference.

The diffraction efficiencies of the incident THz pulse at various frequencies, η, are determined by applying fast Fourier transform algorithms to time-domain waveforms and normalizing the magnitudes of the diffracted signals for o-ray and e-ray with respect to that of the reference. In Figure 5, we plot the diffraction efficiency of the phase grating with the LC driven at different applying voltages as a function of frequency. The experimental results are in good agreements with the theoretical predictions according to Eq. (1). These results clearly demonstrated that the diffraction efficiency of the phase grating was the highest at the frequency of 0.3 THz, according to our design. For ordinary wave at 0.3 THz, the phase difference between fused silica and E7 was close to 2π. Therefore, the transmission of the grating was higher. The THz wave was mainly concentrated in the 0th order. In contrast, the phase difference is close to π for extraordinary waves at 0.3 THz. The diffraction efficiency was smaller for the 0th order, because the THz wave was mostly diffracted into the 1st order.

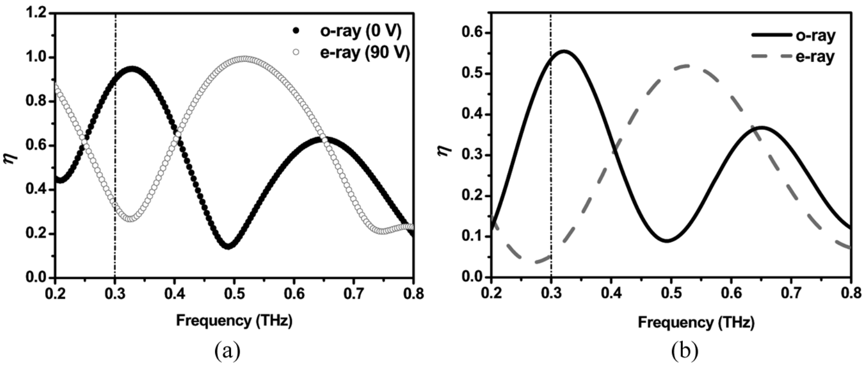

FIGURE 5 (a) Experimental observation and (b) theoretical calculation of diffraction efficiencies of the phase grating as a function of frequency. Curves for the grating driven at two different applied voltages corresponding to o-ray and e-ray are shown.

CONCLUSIONS

We propose and demonstrate an electrically controlled liquid crystal phase grating for the terahertz wave. The performance of the device was characterized by a terahertz time-domain spectrometer. The experimental results were in a good agreement with the theoretic prediction by classic diffraction theory. Applications of the device include beam splitting, scanning, and modulation of the THz wave.

REFERENCES

[1] Ferguson, B. & Zhang, X.-C. (2002). *Nature Materials*, *1*, 26.
[2] Mittleman, D. (2002). *Sensing with THz radiation*, Spring-Verlag: New York.
[3] Siegel, P. H. (2002). *IEEE Trans. Microwave Theory Tech.*, *50*, 910.
[4] Libon, I. H., Baumgärtner, S., Hempel, M., Hecker, N. E., Feldmann, J., Koch, M., & Dawson, P. (2000). *Appl. Phys. Lett.*, *76*, 2821.
[5] Kleine-Ostmann, T., Dawson, P., Pierz, K., Hein, G., & Koch, M. (2004). *Appl. Phys. Lett.*, *84*, 3555.
[6] Kersting, R., Strasser, G., & Unterrainer, K. (2000). *Electron. Lett.*, *36*, 1156.
[7] Tsai, T. R., Chen, C. Y., Pan, C.-L., Pan, R.-P., & Zhang, X.-C. (2003). *Appl. Opt.*, *42*, 2372.
[8] Pan, R.-P., Tsai, T.-R., Chen, C.-Y., & Pan, C.-L. (2003). *J. Biological Physics*, *29*, 335.
[9] Pan, R.-P., Tsai, T.-R., Wang, C., Chen, C.-Y., & Pan, C.-L. (2004). *Mol. Cryst. Liq. Crystl.*, *409*, 137.
[10] Pan, R.-P., Hsieh, C.-F., Pan, C.-L., & Chen, C.-Y. (2008). *J. Appl. Phys.*, *103*, 1.
[11] Tang, T.-T., Pan, R.-P., Wang, Y.-C., & Pan, C.-L. (2008). *Ferroelectrics*, *364*, 72.

[12] Chen, C.-Y., Hsieh, C.-F., Lin, Y.-F., Pan, R.-P., & Pan, C.-L. (2004). *Opt. Express*, *12*, 2625.
[13] Wu, H.-Y., Hsieh, C.-F., Tang, T.-T., Pan, R.-P., & Pan, C.-L. (2006). *IEEE Photon. Technol. Lett.*, *18*, 1488.
[14] Lin, C.-J., Li, Y.-T., Hsieh, C.-F., Pan, R.-P., & Pan, C.-L. (2008). *Optics Express*, *16*, 2995.
[15] Pan, C.-L., Hsieh, C.-F., Pan, R.-P., Tanaka, M., Miyamaru, F., Tani, M., & Hangyo, M. (2005). *Opt. Express*, *13*, 3921.